AIP | Applied Physics Letters

Wireless current sensing by near field induction from a spin transfer torque nano-oscillator

B. Ramaswamy, J. M. Algarin, I. N. Weinberg, Y.-J. Chen, I. N. Krivorotov, J. A. Katine, B. Shapiro, and E. Waks

Citation: Applied Physics Letters **108**, 242403 (2016); doi: 10.1063/1.4953621
View online: http://dx.doi.org/10.1063/1.4953621
View Table of Contents: http://scitation.aip.org/content/aip/journal/apl/108/24?ver=pdfcov
Published by the AIP Publishing

Wireless current sensing by near field induction from a spin transfer torque nano-oscillator

B. Ramaswamy,[1,a)] J. M. Algarin,[2,a)] I. N. Weinberg,[3] Y.-J. Chen,[4] I. N. Krivorotov,[4] J. A. Katine,[5] B. Shapiro,[1,6] and E. Waks[2,b)]
[1]*Fischell Department of Bioengineering, University of Maryland, College Park, Maryland 20742, USA*
[2]*Institute for Research in Electronics and Applied Physics (IREAP), University of Maryland, College Park, Maryland 20742, USA*
[3]*Weinberg Medical Physics LLC, Bethesda, Maryland 20817, USA*
[4]*Department of Physics and Astronomy, University of California, Irvine, California 92697, USA*
[5]*HGST Research Center, San Jose, California 95135, USA*
[6]*Institute for Systems Research (ISR), University of Maryland, College Park, Maryland 20742, USA*

(Received 19 February 2016; accepted 27 May 2016; published online 13 June 2016)

We demonstrate that spin transfer torque nano-oscillators (STNO) can act as wireless sensors for local current. The STNO acts as a transducer that converts weak direct currents into microwave field oscillations that we detect using an inductive coil. We detect direct currents in the range of 300–700 μA and report them wirelessly to a receiving induction coil at distances exceeding 6.5 mm. This current sensor could find application in chemical and biological sensing and industrial inspection. *Published by AIP Publishing.* [http://dx.doi.org/10.1063/1.4953621]

The ability to detect small local currents with high spatial resolution plays an important role in a broad range of applications such as non-destructive testing, industrial electronics, and biosensing. For example, local currents identify the location of defects and malfunctioning circuits in current transformers and complementary metal oxide semiconductor circuits,[1,2] detect mechanical defects,[3] and sense the concentration of polluting gas byproducts of combustion or automotive emission.[4] In biological systems such as the central nervous system, local currents provide information about neuronal activity.[5] The ability to wirelessly detect local currents with high spatial precision is highly desirable for many of these applications. For example, detecting the amplitude and position of currents wirelessly provides information about the activity inside of an organism non-invasively and helps track regions of abnormality.[6,7] In electronic circuits, wireless inspection of defects enables diagnosis without dismantling the whole system.[1]

A number of methods currently exist for detecting currents wirelessly. Magnetic field sensors can detect current flowing by measuring the static magnetic fields they generate.[8,9] Although these methods can detect very low currents, they generally cannot achieve high spatial resolution without placing the sensor very close to the current because magnetometers will detect the sum of the fields from all current sources within their detection range.[8] One way to circumvent this problem is to place a small sensor near the source of the current that reports wirelessly to an external receiver. Although this method requires a direct connection between the sensor and the current source, it can provide very high spatial resolutions while still providing wireless access to the sensor by an external receiver. For example, magnetometers based on diamond nanocrystals can detect local magnetic fields and report them to an external detector via their fluorescence at optical frequencies.[10,11] But optical fields cannot penetrate opaque specimen such as biological tissue and electronic packaging. Methods based on voltage sensitive dyes can also report local current activity with high spatial resolution.[12] But these methods also require optical access.

Spin transfer torque nano-oscillators (STNOs) can provide an alternate approach for detecting local currents. These devices take as their input small direct currents and convert them to microwave current oscillations[13–17] that can report wirelessly to a receiver by magnetic induction. The STNO occupies a small device footprint, potentially in the nanoscale, and can operate with input currents as low as 50 μA (Ref. 18) opening the possibility for detecting weak signals with high spatial precision. Furthermore, the oscillation frequency of the device shifts in the presence of an external magnetic field and current magnitude,[15,19] enabling the precession frequency to encode spatial information in an analogous way to conventional magnetic resonance imaging. These properties make STNOs promising candidates for detecting small currents with high spatial precision. For example, in biological sensing, they could potentially report on electrical activity *in vivo* in areas with no optical access due to the presence of bone or thick tissue.

Previous theoretical works investigated wireless broadcast with spin-transfer torque nano-oscillators for power transfer applications. Amin *et al.*[20] theoretically studied the radiation pattern of these devices and showed that the magnetic field oscillations in a spin-transfer torque nano-oscillator are detectable in the near field. Prokopenko *et al.*[21] evaluated the radiation of arrays of oscillators as efficient sources of microwave signals for telecommunication devices. Experimentally, previous studies demonstrated wireless transmission using a STNO over distances from 10 mm to 1 m,[22,23] with potential applications in wireless communication. However, these works used active amplifiers and large dipole antennas to broadcast the signal. Such amplifiers and large antennas are appropriate for communication, but are difficult to integrate into small wireless sensors and require

[a)]B. Ramaswamy and J. M. Algarin contributed equally to this work.
[b)]Author to whom correspondence should be addressed. Electronic mail: edowaks@umd.edu.

wireless power supplies which are challenging to fabricate. Many sensing applications often require compact passive sensors without any power sources beyond the local currents. To date, such wireless sensing of currents using a STNO has not been experimentally demonstrated.

Here, we report direct wireless sensing of local currents by magnetic induction using a STNO. We use a microfabricated receiving coil to detect the microwave oscillations produced by the device, and detect currents in the range of 300–700 μA at distances of up to 6.5 mm. These results show that spintronic devices could potentially serve as nanoscale sensors for applications in biotechnology, electronics, and embedded systems.

The devices studied in this work are elliptical magnetic tunnel junction nanopillars with lateral dimensions 70 nm × 170 nm. Fig. 1(a) shows the complete layer structure for the device, with thicknesses indicated in parentheses in units of nanometers. We deposited all layers using magnetron sputtering in a Singulus TIMARIS system and patterned the magnetic tunnel junctions using electron beam lithography followed by ion milling. The synthetic antiferromagnet is PtMn(15)/$Co_{70}Fe_{30}$(2.3)/Ru(0.85)/$Co_{40}Fe_{40}B_{20}$(2.4) with the $Co_{70}Fe_{30}$ pinned layer and the $Co_{40}Fe_{40}B_{20}$ reference layer antiferromagnetically coupled by the tuned thickness of Ru. Prior to patterning, we anneal the multilayer for 2 h at 300 °C in a 1 T in-plane field to set the pinned layer exchange bias direction parallel to the long axis of the nanopillars.

To perform wireless current sensing, we utilize the experimental configuration illustrated in Fig. 1(b). We inject the direct current signal into the device using a non-magnetic picoprobe (10-50/30-125-BeCu-2-R-200, GGB industries). This direct current flows from the free layer to the fixed layer of the device (Fig. 1(c)). We apply a magnetic field of 0.15 T using a permanent magnet (K&J Magnetics) at an out-of-plane angle of 60° with respect to the sample plane and an in-plane component of 30° with respect to the major axis of the ellipse, which induces a free-layer precession[18] at a frequency of $f = 2.7$ GHz. The fixed layer and free layer are oriented mostly anti-parallel in the applied field conditions,[24] and the observed oscillation mode is likely the lowest-frequency free layer mode in the anti-parallel state.[26] The free layer precession generates a microwave frequency electromagnetic signal across the oscillator terminals via a tunneling magnetoresistance effect.[25,26] The microwave signal inductively couples to a receiving micro-coil, resulting in a microwave voltage detected across the terminals of the coil. We also use a bias tee (Pasternack, PE1604) to extract the microwave at the output of the device using the capacitive port, which we can compare to the wireless induction signal. The magnitude of this microwave signal depends on the amount of direct current injected to the device, while the resonant frequency depends on the magnitude and direction of the external magnetic field applied as well as on the direct current injected to the device.

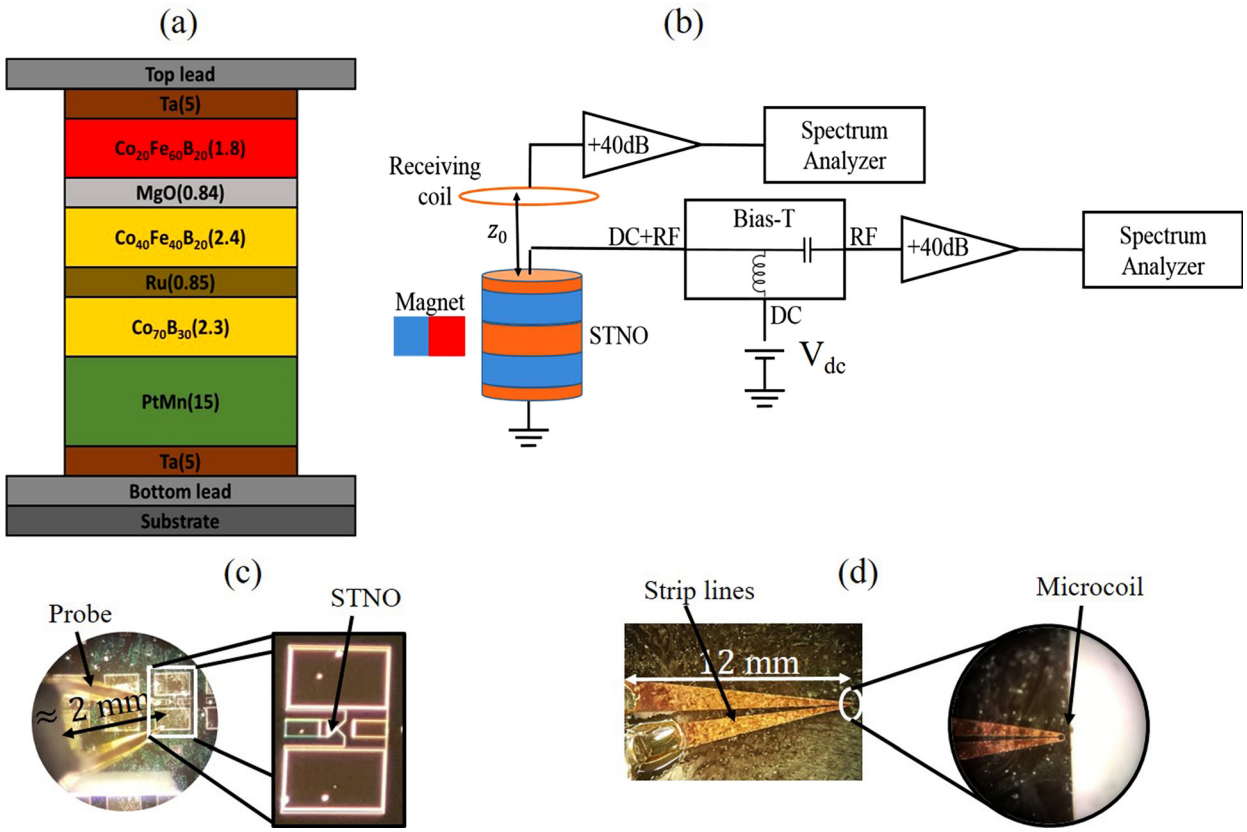

FIG. 1. (a) Schematic of the nanopillar spin torque oscillator device. The numbers in parentheses are the layer thicknesses in units of nanometers. (b) A schematic of the microwave circuit used for direct electrical measurement from the device and wireless measurement of the microwave signal emission from STNO. (c) The microprobe and the connection pads along with the spin torque nano-oscillator forming an effective inductive coupler. (d) The microfabricated receiving coil patterned on SiO_2 substrate.

The receiving micro-coil, shown in Fig. 1(d), is composed of a metallic loop antenna with outer diameter of 46 μm and width of 6 μm. We fabricated the receiving coil on a SiO_2 substrate using optical lithography followed by thermal vapor deposition of copper (thickness of 0.5 μm) and liftoff. We position the receiving coil directly above the device surface with the patterned coil facing the device. This is to ensure that the substrate thicknesses do not limit the distance between the device and the coil. We collect the current from the coil using a strip line as a matching network to match the coil impedance to 50 Ω and a coaxial SMA connector directly soldered to the leads of the strip line. A low noise amplifier (Pasternack PE15A1010, gain = 40 dB and input impedance = 50 Ω) amplifies the output from the coil. We analyze the amplified output using a spectrum analyzer (Agilent 8564 EC). We used the same spectrum analyzer to measure the output of the device through the capacitive port of the bias tee, so that we can compare the signals under identical conditions.

Fig. 2(a) shows the power spectral density of the device output collected from the bias tee for different values of the direct input current. The device begins to oscillate at an input current of approximately 100 μA with an oscillation frequency of 2.75 GHz. The oscillation frequency decreases as we increase the input current, which is expected because the nonlinear frequency shift for this device geometry is negative.[15,19] At 600 μA, the device approaches the maximum output power spectral density of 400 nW/GHz. At even larger input current of 700 μA, we observe a second oscillation mode at a slightly lower frequency which results in a broadened spectrum with two peaks. We attribute the lower frequency mode to the onset of the spin-torque-driven auto-oscillation mode[19,24] while the higher frequency mode is likely due to thermally activated oscillations.[27] Either signal can be used to perform sensing and the choice mainly depends on the amplitude of the input current.

Fig. 2(b) shows the power spectrum of the induction signal obtained from the receiving coil for the same input currents used in Fig. 2(a). In these measurements, we position the receiving coil at a distance of 15 μm above the device. The spectra through the coil match the electrical measurements directly from the device shown in Fig. 2(a). We attribute the difference in the spectral shapes of the induced signal and the direct electrical signal to a mismatch between the frequency response of the device and the receiving coil. We attain a peak signal power density of 1.7 nW/GHz, which is a factor of 300 smaller than the measurement from the capacitive port of the bias tee. We note that the capacitive port of the bias tee shows microwave signal at input currents as low as 100 μA, but the wireless induction signal requires 300 μA to be detectable with our measurement setup. This disparity is caused by the reduced signal in the induction coil, which requires more driving current to generate a signal that exceeds the noise floor of the electrical circuit. We also note that the lower frequency mode (which appears at an input current 700 μA) induces signal more efficiently in the receiving coil, due to better spectral matching with the coil. We further confirmed this by measuring the transmission characteristics between the coil and the device using a vector network analyzer as explained in later paragraphs. As shown in Fig. 2(b) inset, the transmission coefficient is higher for

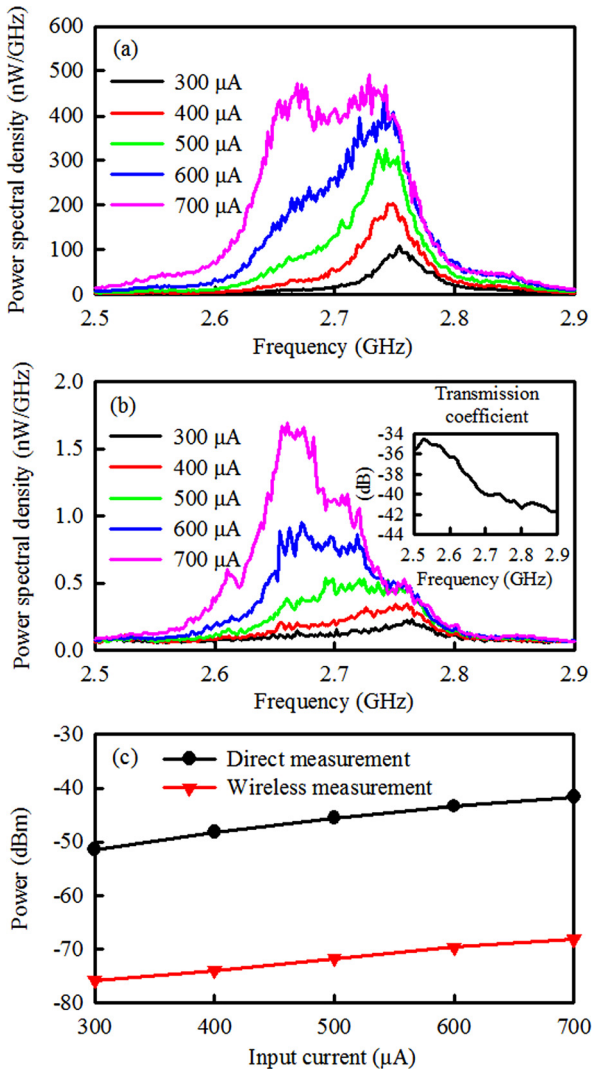

FIG. 2. (a) The power spectral density of the direct electrical signal measured from the STNO at 0.15 T. (b) The power spectral density of the wireless signal measured from the receiving coil at 0.15 T. The transmission coefficient measured between the device and coil using a network analyzer for the same frequency range (inset). (c) The integrated power obtained in measurements versus bias current (a) and (b).

the lower frequency mode of 2.66 GHz compared to the higher frequency mode of 2.73 GHz.

Fig. 2(c) plots the total microwave power for both the electrical output of the bias tee and the wireless signal induced in the receiving coil. Both signals exhibit the expected behavior where the microwave power increases with increased current.[28] Furthermore, the input current dependence of the wireless signal shows an identical behavior to the electrical measurement from the bias tee, which confirms that the wireless signal originates from the current induced in the device. At a maximum input current of 700 μA, the electrical power measured directly from the bias tee is 69 nW, as shown in Fig. 2(c). However, due to the impedance mismatch between the device and the amplifier, the measured electrical power from the bias tee is not the total power produced in the device. The total power produced in the device, P_d, is given by[29]

$$P_d = \frac{Z_0 + Z_d}{Z_0} P_e, \tag{1}$$

where P_e is the electrical power measured in the spectrum analyzer, $Z_d = 1$ kΩ is the impedance of the device, and $Z_0 = 50$ Ω is the input impedance of the amplifier connected to the device. From Eq. (1), the total power produced in the device is 1449 nW. The wireless signal power measured in the receiving coil at maximum input current of 700 μA is 0.15 nW, as shown in Fig. 2(c). The transmission efficiency defined as the ratio between the wireless power received in the coil and the power generated by the device is 0.01%. Fig. 3 plots the total power in the receiving coil as a function of distance between the receiving coil and the surface of the device, where we fix the input current at 700 μA. We observe a clear induction signal at distances of up to 6.5 mm.

The STNO can induce current in the receiving micro-coil through two different mechanisms. The first is by direct induction from precessing magnetization of the free layer, and the second is induction by the microwave current oscillation in the electrical wires that connect to the device. A calculation of the power directly induced by the precessing magnetization of the free layer indicates a value 8 orders of magnitude smaller than the actual signal we detect (see the supplementary material). Thus, the dominant mechanism for induction is through the electrical wires that connect to the device.

The induced power due to the microwave current oscillations in the device depends upon the geometry of the connecting pads, wires surrounding the device, and the microwave probe that contacts it. These wires form an effective inductive coupler that can induce current in the receiver. We performed numerical simulations using CST Microwave Studio (Computer Simulation Technology, Inc.) to determine the induced power in the receiving micro-coil by this effective inductive coupler. These simulations incorporate the receiving micro-coil with its corresponding strip lines (see Fig. 1(d)) connected to a port of impedance 50 Ω. We model the device as a port of impedance 1 k Ω. We include the pads connected to the device along with the input probe (see Fig. 1(c)), and add a series resistance of 50 Ω to the probe to account for the impedance of the amplifier connected to the probe. From the numerical simulations, we calculate an induced power of $P = 0.05$ nW in the receiving coil, which is close to our measured value of $P = 0.15$ nW, suggesting that the wireless power received is due to the microwave current oscillation in wires connecting to the device. The remaining discrepancy between the measured and numerically calculated values is likely due to the simplification of the complex probe geometry in our model.

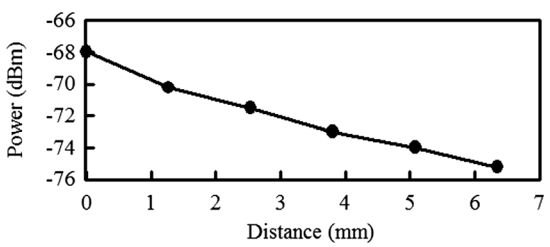

FIG. 3. The wireless signal received from the STNO as a function of distance between the STNO and the receiving coil for a detection current I_{DC} = 700 μA.

To further validate that the wireless induction signal originates from the microwave current oscillations in the device, we use a two port network analyzer (Hewlett Packard 8722D, 50 MHz–40 GHz) to estimate the transmission efficiency between the device and the receiver and compare it with the value previously calculated from the measurements in the spectrum analyzer. We connect the port one of the network analyzer to the device and the port two to the receiving coil with the coil placed directly above the device as explained before. For simplicity, we assume that the receiver is perfectly matched to 50 Ω (due to the matching network) and that the main power is dissipated in the device (which is a good assumption due to its high impedance). With these assumptions, the transmission efficiency, η, can be estimated from the scattering parameters as[29]

$$\eta = \frac{Z_d}{Z_d + Z_0} \frac{|S_{21}|^2}{1 - |S_{11}|^2}, \tag{2}$$

where $Z_d = 1$ kΩ is the impedance of the device, $Z_0 = 50$ Ω is the input impedance of the amplifier connected to the device, S_{11} is the reflection coefficient in the device, and S_{21} is the transmission coefficient between the device and the receiving coil. We measured the scattering parameters at 2.7 GHz, to be $S_{11} = -1.22$ dB and $S_{21} = -39.95$ dB. Introducing these values into Eq. (2), we estimate a transmission efficiency of 0.04%. This value approximates the transmission efficiency of 0.01% observed in our previous experiment of wireless detection from the device.

In summary, we have demonstrated that STNOs can act as wireless sensors for small local currents. We detected current and reported it wirelessly at distances exceeding 6 mm from the STNO. We could improve the current sensitivity by using STNOs with lower threshold currents.[18] Non-adiabatic stochastic resonance of magnetization[30,31] could also improve the sensitivity of the measurement by enhancing the amplitude of magnetization precession for a small current input. In addition, the current device uses the contact wires on the chip as an effective inductive coupler, which has a small mutual inductance with the receiving coil. We could increase the detection distance by patterning inductors on the device itself that have higher mutual inductance with the receiver. Devices with large-amplitude magnetization precession,[32,33] reduced phase noise,[34] arrays of phase locked oscillators,[35–37] or oscillators with large volume of the free magnetic layer[38] could further extend the sensing range by emitting more power in a narrower bandwidth. Ultimately, our results present an approach for wireless current sensing that may play an important role in embedded systems, non-destructive testing of electronics, and in-vivo biological sensing and imaging.

See supplementary material for the calculation of power directly induced by the precessing magnetization of the free layer of the STNO in the receiving micro-coil.

We thank Dr. John Rodgers and Bisrat Adissie for providing access to the microwave equipment. We thank Juergen Langer and Berthold Ocker for magnetic multilayer deposition. We also gratefully acknowledge support from a NSF BRAIN EAGER grant (Grant No. DBI1450921) as part of the

BRAIN initiative. The work of Yu-Jin Chen and Ilya Krivorotov on sample design and characterization was supported as part of the SHINES, an Energy Frontier Research Center funded by the U.S. Department of Energy, Office of Science, Basic Energy Sciences under Award No. # SC0012670.

[1]S. Ziegler, R. C. Woodward, H. H.-C. Iu, and L. J. Borle, IEEE Sens. J. **9**, 354 (2009).
[2]D. B. I. Feltham, P. J. Nigh, L. R. Carley, and W. Maly, in *Proceedings of the 1988 IEEE International Conference on Computer Design: VLSI in Computers and Processors, 1988 (ICCD 88)* (1988), pp. 454–457.
[3]H. K. Akira Todoroki and K. Matsuura, in *Proceedings of the 10th International Conference on Composite Materials* (Woodhead Publishing, 1995), p. 323.
[4]J. Kong, N. R. Franklin, C. Zhou, M. G. Chapline, S. Peng, K. Cho, and H. Dai, Science **287**, 622 (2000).
[5]G. Buzsáki, C. A. Anastassiou, and C. Koch, Nat. Rev. Neurosci. **13**, 407 (2012).
[6]D. J. Heeger and D. Ress, Nat. Rev. Neurosci. **3**, 142 (2002).
[7]A. M. Cassará, B. Maraviglia, S. Hartwig, L. Trahms, and M. Burghoff, Magn. Reson. Imaging **27**, 1131 (2009).
[8]J. Lenz and A. S. Edelstein, IEEE Sens. J. **6**, 631 (2006).
[9]S. Nakayama and T. Uchiyama, Sci. Rep. **5**, 8837 (2015).
[10]J. M. Taylor, P. Cappellaro, L. Childress, L. Jiang, D. Budker, P. R. Hemmer, A. Yacoby, R. Walsworth, and M. D. Lukin, Nat. Phys. **4**, 810 (2008).
[11]G. Balasubramanian, I. Y. Chan, R. Kolesov, M. Al-Hmoud, J. Tisler, C. Shin, C. Kim, A. Wojcik, P. R. Hemmer, A. Krueger, T. Hanke, A. Leitenstorfer, R. Bratschitsch, F. Jelezko, and J. Wrachtrup, Nature **455**, 648 (2008).
[12]S. Chemla and F. Chavane, J. Physiol. (Paris) **104**, 40 (2010).
[13]W. H. Rippard, M. R. Pufall, S. Kaka, S. E. Russek, and T. J. Silva, Phys. Rev. Lett. **92**, 027201 (2004).
[14]A. M. Deac, A. Fukushima, H. Kubota, H. Maehara, Y. Suzuki, S. Yuasa, Y. Nagamine, K. Tsunekawa, D. D. Djayaprawira, and N. Watanabe, Nat. Phys. **4**, 803 (2008).
[15]S. I. Kiselev, J. C. Sankey, I. N. Krivorotov, N. C. Emley, R. J. Schoelkopf, R. A. Buhrman, and D. C. Ralph, Nature **425**, 380 (2003).
[16]D. Houssameddine, S. H. Florez, J. A. Katine, J.-P. Michel, U. Ebels, D. Mauri, O. Ozatay, B. Delaet, B. Viala, L. Folks, B. D. Terris, and M.-C. Cyrille, Appl. Phys. Lett. **93**, 022505 (2008).
[17]Y. Zhou, C. L. Zha, S. Bonetti, J. Persson, and J. Åkerman, Appl. Phys. Lett. **92**, 262508 (2008).
[18]Z. Zeng, G. Finocchio, B. Zhang, P. Khalili Amiri, J. A. Katine, I. N. Krivorotov, Y. Huai, J. Langer, B. Azzerboni, K. L. Wang, and H. Jiang, Sci. Rep. **3**, 1426 (2013).
[19]A. Slavin and V. Tiberkevich, IEEE Trans. Magn. **45**, 1875 (2009).
[20]N. Amin, H. Xi, and M. X. Tang, IEEE Trans. Magn. **45**, 4183 (2009).
[21]O. Prokopenko, E. Bankowski, T. Meitzler, V. Tiberkevich, and A. Slavin, IEEE Magn. Lett. **2**, 3000104 (2011).
[22]H. S. Choi, S. Y. Kang, S. J. Cho, I.-Y. Oh, M. Shin, H. Park, C. Jang, B.-C. Min, S.-I. Kim, S.-Y. Park, and C. S. Park, Sci. Rep. **4**, 5486 (2014).
[23]I. Oh, S. Park, D.-H. Kang, and C. S. Park, IEEE Microwave Wireless Compon. Lett. **24**, 502 (2014).
[24]P. K. Muduli, O. G. Heinonen, and J. Åkerman, Phys. Rev. B **83**, 184410 (2011).
[25]W. H. Butler, X.-G. Zhang, T. C. Schulthess, and J. M. MacLaren, Phys. Rev. B **63**, 054416 (2001).
[26]S. Ikeda, K. Miura, H. Yamamoto, K. Mizunuma, H. D. Gan, M. Endo, S. Kanai, J. Hayakawa, F. Matsukura, and H. Ohno, Nat. Mater. **9**, 721 (2010).
[27]B. Georges, J. Grollier, V. Cros, A. Fert, A. Fukushima, H. Kubota, K. Yakushijin, S. Yuasa, and K. Ando, Phys. Rev. B **80**, 060404 (2009).
[28]Z. Zeng, P. K. Amiri, I. N. Krivorotov, H. Zhao, G. Finocchio, J.-P. Wang, J. A. Katine, Y. Huai, J. Langer, K. Galatsis, K. L. Wang, and H. Jiang, ACS Nano **6**, 6115 (2012).
[29]D. M. Pozar, *Microwave Engineering*, 4th ed. (Wiley Global Education, 2011).
[30]X. Cheng, C. T. Boone, J. Zhu, and I. N. Krivorotov, Phys. Rev. Lett. **105**, 047202 (2010).
[31]X. Cheng, J. A. Katine, G. E. Rowlands, and I. N. Krivorotov, Appl. Phys. Lett. **103**, 082402 (2013).
[32]H. Maehara, H. Kubota, Y. Suzuki, T. Seki, K. Nishimura, Y. Nagamine, K. Tsunekawa, A. Fukushima, A. M. Deac, K. Ando, and S. Yuasa, Appl. Phys. Express **6**, 113005 (2013).
[33]G. E. Rowlands and I. N. Krivorotov, Phys. Rev. B **86**, 094425 (2012).
[34]L. Yang, R. Verba, V. Tiberkevich, T. Schneider, A. Smith, Z. Duan, B. Youngblood, K. Lenz, J. Lindner, A. N. Slavin, and I. N. Krivorotov, Sci. Rep. **5**, 16942 (2015).
[35]S. Kaka, M. R. Pufall, W. H. Rippard, T. J. Silva, S. E. Russek, and J. A. Katine, Nature **437**, 389 (2005).
[36]S. Tamaru, H. Kubota, K. Yakushiji, S. Yuasa, and A. Fukushima, Sci. Rep. **5**, 18134 (2015).
[37]Y. Zhou, J. Persson, S. Bonetti, and J. Åkerman, Appl. Phys. Lett. **92**, 092505 (2008).
[38]Z. Duan, A. Smith, L. Yang, B. Youngblood, J. Lindner, V. E. Demidov, S. O. Demokritov, and I. N. Krivorotov, Nat. Commun. **5**, 5616 (2014).